

# The Bose-Fermi duality in quantum Otto heat engine with trapped repulsive Bosons

Jinfu Chen,<sup>1,2</sup> Hui Dong,<sup>2,\*</sup> and Chang-Pu Sun<sup>1,2,†</sup>

<sup>1</sup>Beijing Computational Science Research Center, Beijing 100193, China

<sup>2</sup>Graduate School of China Academy of Engineering Physics,

No. 10 Xibeiwang East Road, Haidian District, Beijing, 100193, China

(Dated: July 8, 2022)

Quantum heat engine with ideal gas has been well studied, yet the role of interaction was seldom explored. We construct a quantum Otto heat engine with  $N$  repulsive Bosonic particles in a 1D hard wall box. With the advantage of exact solution using Bethe Ansatz, we obtain not only the exact numerical result of efficiency in all interacting strength  $c$ , but also analytical results for strong interaction. We find the efficiency  $\eta$  recovers to the one of non-interacting case  $\eta_{\text{non}} = 1 - (L_1/L_2)^2$  for strong interaction with asymptotic behavior  $\eta \sim \eta_{\text{non}} - 4(N-1)L_1(L_2 - L_1)/(cL_2^3)$ . Here,  $L_1$  and  $L_2$  are two trap sizes during the cycle. Such recovery reflects the duality between 1D strongly repulsive Bosons and free Fermions. We observe and explain the appearance of a minimum efficiency at a particular interacting strength  $c$ , and study its dependence on the temperature.

## I. INTRODUCTION

In classical thermodynamics, piston model with ideal gas serves as a prototype to realize heat engines with the different cycles, such as Carnot and Otto cycle [1, 2]. The non-interacting gas makes it feasible to obtain very simple results for efficiency as well as other properties [1]. Such simplicity also enables direct extensions of similar discussions in quantum region to show unique features of quantum thermodynamics with single particle as well as few identical particles without interaction [3–8]. The difficulty arises when the interaction between particles is considered for a quantum heat engine. Recently, Bengtsson et.al explores the effect of the attractive interaction with exact numerical simulation and show the increase of work output in the Szilard engine [9]. However, it remains unclear how the work conversion is affected by interactions in the widely used heat engine cycles, e.g., quantum Otto cycle.

In order to show the effect of interaction on the efficiency, we construct a quantum Otto heat engine with 1D repulsive Bose gas in a hard wall box [10–12]. Quantum Otto cycle is a simple and feasible cycle in quantum thermodynamics [3, 13], and has been studied concretely in many quantum systems [14–19]. The advantage of our model is its exact solution with Bethe’s ansatz [10, 20], which allows the analytical results to show the effect of interaction in quantum thermodynamics. We find that the efficiency of the heat engine first decreases, reaches to the minimum value and finally recovers to the initial value along with the increasing of the interacting strength  $c$ . For strong interacting strength, the recovery of the efficiency is explained by the Bose-Fermi duality [21]. We observe a dip for the efficiency with particular interacting strength. We also study how temperature affects the dip of the efficiency.

This paper is organized as follows. In Sec. II, we introduce the solution of 1D interacting Bose gas in a hard wall box by Bethe ansatz, and build the quantum Otto heat engine on this model. In Sec. III, we give the asymptotic efficiency for large interacting strength and the numerical efficiency for any interacting strength. The recovery of the efficiency for large interacting strength reflects the Bose-Fermi duality between 1D strongly repulsive Bosons and free Fermions. We associate the efficiency with the ratio for different state, and study the efficiency for different temperature.

## II. OTTO ENGINE WITH REPULSIVE BOSONS

In this section, we design a quantum Otto heat engine with 1D repulsive Bose gas in a hard wall box. The efficiency of the quantum Otto cycle for different interacting strength  $c$  is studied to explore the effect of the interaction on the quantum heat engine.

The Hamiltonian for  $N$  repulsive Bosonic particles in a 1D hard wall box is

$$H(L, c) = \sum_{i=1}^N \frac{p_i^2}{2m} + \frac{c}{m} \sum_{i<j} \delta(x_i - x_j) + V(\{x_i\}), \quad (1)$$

where  $p_i$  and  $x_i$  are the momentum and coordinate for  $i$ -th particle with mass  $m$ . The interacting strength  $c$  is positive for repulsive interaction. The trap potential  $V(\{x_i\})$  is infinite square potential

$$V(\{x_i\}) = \begin{cases} 0 & \forall 0 \leq x_i \leq L \\ \infty & \exists x_i < 0, \text{ or } x_i > L. \end{cases} \quad (2)$$

Eigenstates can be obtained with Bethe Ansatz [10] for the current trap. The eigenstate is written as  $\psi_{\{k_i\}}(\{x_i\}) = \sum_P a(P) \exp(i \sum_{l=1}^N k_{P(l)} x_l)$ ,  $0 \leq x_1 \leq x_2, \dots \leq x_N \leq L$ , with the superposition coefficient  $a(P)$ . We are interested in the thermodynamic property and skip the concrete form of  $a(P)$ , whose explicit form can

\* hdong@gscaep.ac.cn

† cpsun@csrc.ac.cn

be found in Ref. [10]. The boundary condition gives the self-consistent equation for the wave vectors as

$$k_i L = \pi n_i + \sum_{j \neq i} \left( \arctan \frac{c}{k_i - k_j} + \arctan \frac{c}{k_i + k_j} \right). \quad (3)$$

The eigenstate  $|\{n_i\}\rangle$  is represented by a set of ordered number  $1 \leq n_1 \leq n_2 \leq \dots \leq n_N$ , and the wave vectors satisfy  $1 < k_1 < k_2 < \dots < k_N$ . The corresponding energy for the eigenstate  $|\{n_i\}\rangle$  is

$$E_{\{n_i\}}^{(L)} = \frac{1}{2m} \sum_{i=1}^N k_i^2. \quad (4)$$

With the certain trap size  $L$  and interacting strength  $c$ , the density matrix for the system at the equilibrium state with temperature  $T$  is  $\rho = \sum_{\{n_i\}} p_{\{n_i\}}(T, L, c) |\{n_i\}\rangle \langle \{n_i\}|$ . The probability  $p_{\{n_i\}}(T, L, c)$  on the eigenstate  $|\{n_i\}\rangle$  is

$$p_{\{n_i\}}(T, L, c) = \frac{e^{-\frac{E_{\{n_i\}}^{(L)}}{k_B T}}}{Z(T, L, c)}, \quad (5)$$

with the partition function  $Z(T, L, c) = \sum_{\{n_i\}} \exp[-E_{\{n_i\}}^{(L)}/k_B T]$ . The internal energy of the system is  $U(T, L, c) = \sum_{\{n_i\}} p_{\{n_i\}} E_{\{n_i\}}^{(L)}$ .

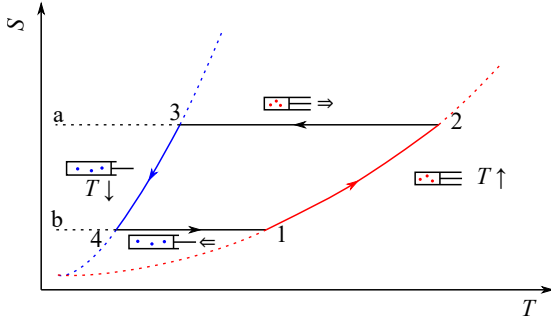


Figure 1. (Color online) Entropy-temperature ( $S - T$ ) diagram for quantum Otto heat engine. The red and blue solid lines are isochoric processes contacting to the cold and hot reservoir with the corresponding trap size as  $L_1$  and  $L_2$ , while the black solid lines are adiabatic processes.

The Otto cycle consists four strokes similar to the single particle Otto cycle [3], illustrated on  $S - T$  diagram in Figure 1. Here, the entropy is evaluated with the von Neumann entropy  $S = -\text{Tr}[\rho \ln \rho]$  for all later discussions. The four strokes are specified as follows,

- Stroke I ( $1 \rightarrow 2$ ): Isochoric heating. Initially, the system does not necessarily stay at equilibrium thermal state. The internal energy of the system at state 1 is  $U_1 = \sum_{\{n_i\}} p_{\{n_i\}}^{(1)} E_{\{n_i\}}^{(L_1)}$ . With the fixed trap size  $L_1$ , the temperature increases slowly enough to allow the system in thermal equilibrium

state with temperature  $T_2$ . The internal energy at state 2 is  $U_2 = \sum_{\{n_i\}} p_{\{n_i\}}^{(2)} E_{\{n_i\}}^{(L_1)}$  with the equilibrium occupation  $p_{\{n_i\}}^{(2)} = p_{\{n_i\}}(T_2, L_1, c)$ . The internal energy increases by absorbing heat from the hot reservoir  $Q_1 = U_2 - U_1 > 0$ .

- Stroke II ( $2 \rightarrow 3$ ): Quantum adiabatic expansion. During the process, the system is isolated from any reservoir, and the trap size increases from  $L_1$  to  $L_2$  slowly in order to keep the occupation number unchanged, namely  $p_{\{n_i\}}^{(3)} = p_{\{n_i\}}^{(2)}$ . In this process, the internal energy decreases from  $U_2 = \sum_{\{n_i\}} p_{\{n_i\}}^{(2)} E_{\{n_i\}}^{(L_1)}$  to  $U_3 = \sum_{\{n_i\}} p_{\{n_i\}}^{(3)} E_{\{n_i\}}^{(L_2)}$  to export work  $W_1 = U_3 - U_2 = \sum_{\{n_i\}} p_{\{n_i\}}^{(2)} (E_{\{n_i\}}^{(L_2)} - E_{\{n_i\}}^{(L_1)}) < 0$ . After the expansion, the system reaches generally a non-equilibrium state, except that the energy levels shift homogeneously.
- Stroke III ( $3 \rightarrow 4$ ): Isochoric cooling. Similar to stroke I, the trap size is fixed at  $L_2$ . The temperature decreases slowly enough to allow the system in thermal equilibrium state with temperature  $T_4$ . The occupation is  $p_{\{n_i\}}^{(4)} = p_{\{n_i\}}(T_4, L_2, c)$ , and the internal energy is  $U_4 = \sum_{\{n_i\}} p_{\{n_i\}}^{(4)} E_{\{n_i\}}^{(L_2)}$ . The internal energy decreases by releasing heat to the cold reservoir  $Q_2 = U_4 - U_3 < 0$ .
- Stroke IV ( $4 \rightarrow 1$ ): Quantum adiabatic compressing. Similar to stroke II, the system is isolated from any reservoir, and the trap size decreases from  $L_2$  to  $L_1$  slowly to keep the probability  $p_{\{n_i\}}$  as a constant, namely,  $p_{\{n_i\}}^{(1)} = p_{\{n_i\}}^{(4)}$ . The system reaches a non-equilibrium state as the initial state of stroke I. The internal energy increases by performed work  $W_2 = U_1 - U_4 = \sum_{\{n_i\}} p_{\{n_i\}}^{(4)} (E_{\{n_i\}}^{(L_1)} - E_{\{n_i\}}^{(L_2)}) > 0$ .

The extracted work for the quantum Otto cycle  $W_{out} = -W_1 - W_2 = Q_1 - |Q_2|$  should be positive to ensure a valid heat engine instead of refrigerator. For ideal gas, the positive work condition gives the requirement  $T_2 > (L_2/L_1)^2 T_4$  [3]. Such condition for repulsive Bosons is complicated without a simple formula. Yet, in all later discussion, we carefully choose the temperature  $T_2, T_4$  to allow the positive work.

The efficiency  $\eta = 1 - |Q_2|/Q_1$  is written explicitly as

$$\eta = \frac{\sum_{\{n_i\}} \left( p_{\{n_i\}}^{(2)} - p_{\{n_i\}}^{(4)} \right) \left( E_{\{n_i\}}^{(L_1)} - E_{\{n_i\}}^{(L_2)} \right)}{\sum_{\{n_i\}} \left( p_{\{n_i\}}^{(2)} - p_{\{n_i\}}^{(4)} \right) E_{\{n_i\}}^{(L_1)}}. \quad (6)$$

In the following numerical calculations, we use Eq. (6) to calculate the exact efficiency.

### III. THE EFFICIENCY AND THE INTERACTION

For the large interacting strength  $c$ , we have the expansion of Eq. (3) to the first order of  $1/c$

$$k_i L = \pi(n_i + i - 1) + \sum_{j \neq i} \left( \frac{k_i - k_j}{c} + \frac{k_i + k_j}{c} \right). \quad (7)$$

The solution for the wave vector is  $k_i = \pi(n_i + i - 1) / (L + 2(N - 1)/c)$ . Eq. (4) gives the asymptotic energy for the eigenstate  $|\{n_i\}\rangle$  as

$$E_{\{n_i\}}^{(L)} = \frac{\pi^2 \sum_{i=1}^N (n_i + i - 1)^2}{2m \left( L + \frac{2(N-1)}{c} \right)^2}. \quad (8)$$

For the large interacting strength, the energy ratios for eigenstates with different trap size have the same value

$$\frac{E_{\{n_i\}}^{(L_2)}}{E_{\{n_i\}}^{(L_1)}} = \left( \frac{L_1 + \frac{2(N-1)}{c}}{L_2 + \frac{2(N-1)}{c}} \right)^2. \quad (9)$$

Therefore, the internal energy for the initial state and the final state of the quantum adiabatic processes has the same ratio as

$$\frac{U_3}{U_2} = \frac{U_4}{U_1} = \left( \frac{L_1 + \frac{2(N-1)}{c}}{L_2 + \frac{2(N-1)}{c}} \right)^2. \quad (10)$$

By Eq. (6), we obtain the efficiency as

$$\eta = 1 - \left( \frac{L_1 + \frac{2(N-1)}{c}}{L_2 + \frac{2(N-1)}{c}} \right)^2. \quad (11)$$

At the large interaction limit, we expand Eq. (11) to get an asymptotic efficiency to the first order of  $1/c$

$$\eta \approx 1 - \left( \frac{L_1}{L_2} \right)^2 - \frac{4L_1(L_2 - L_1)(N - 1)}{L_2^3 c}. \quad (12)$$

Such efficiency matches the one of non-interacting Fermions/Bosons, which is the same for one-single particle quantum Otto heat engine [3]. The recovery the efficiency at strong coupling limit to the ideal gas is caused by the duality between Fermions and Bosons at 1D case [10]. Such duality shows the match between energy levels of strong repulsive interacting Bosons and non-interacting Fermions, or verse vice.

To validate our result in Eq. (11, 12), we compare it to the exact numerical result in Fig. 2. The efficiency for heat engine with different numbers  $N = 2, 3, 4$  of Bosons are plotted as functions of interacting strength  $c$ . In the simulation, we set the mass  $m = 1$ , and choose a cutoff  $n_{\text{cut}} = 20$  for the energy level index  $n_i$ , namely,  $n_i \leq n_{\text{cut}}$ . For the exact numerical calculation, we firstly

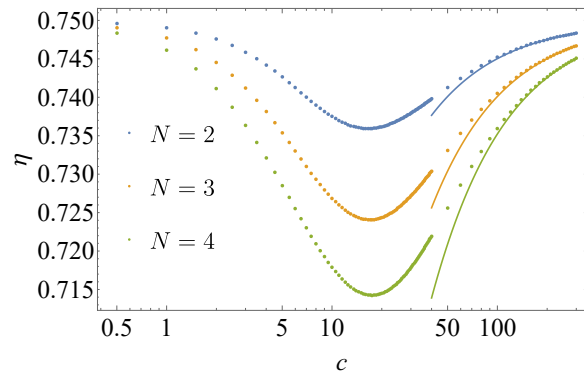


Figure 2. (Color online) the log-linear plot for the efficiency  $\eta$  for the quantum Otto heat engine with different interacting strength  $c$ . We consider three cases with the particle number as  $N = 2, 3, 4$ , and choose the temperature as  $T_2 = 50, T_4 = 8$ . For all numerical calculation, the mass and the cutoff of the quantum number are set as  $m = 1$  and  $n_{\text{cut}} = 20$ , and the trap size is always set as  $L_1 = 1, L_2 = 2$ . The solid line is the analytical result of the asymptotic efficiency for large  $c$  by Eq. (8), while the dots are the exact numerical result.

calculate the energy levels  $E_{\{n_i\}}^{(L_1)}$  and  $E_{\{n_i\}}^{(L_2)}$  by exactly solving Eq. (3) with the trap size as  $L_1 = 1$  and  $L_2 = 2$ . Next, we calculate the probability  $p_{\{n_i\}}^{(2)}$  and  $p_{\{n_i\}}^{(4)}$  for the equilibrium state 2 and 4 with the temperature  $T_2 = 50$  and  $T_4 = 8$  for the hot and cold reservoir respectively. And the exact efficiency is evaluated via Eq. (6) with the probability  $p_{\{n_i\}}^{(i)}$  and the energy levels  $E_{\{n_i\}}^{(L_i)}$ . In Fig 2, we show that the numerical result matches the analytical result by Eq. (11) well for the large interacting strength,

Interestingly, the curve for efficiency shows a dip with particular interacting strength  $c$  in Fig. 2. To understand the appearance of such dip, we rewrite the efficiency in Eq. (6) as

$$\eta = \frac{\sum_{\{n_i\}} \left( p_{\{n_i\}}^{(2)} - p_{\{n_i\}}^{(4)} \right) E_{\{n_i\}}^{(L_1)} \lambda_{\{n_i\}}(L_1, L_2)}{\sum_{\{n_i\}} \left( p_{\{n_i\}}^{(2)} - p_{\{n_i\}}^{(4)} \right) E_{\{n_i\}}^{(L_2)}}, \quad (13)$$

where  $\lambda_{\{n_i\}}(L_1, L_2) = 1 - E_{\{n_i\}}^{(L_2)} / E_{\{n_i\}}^{(L_1)}$  is a ratio, similar to the Otto efficiency for a two-level heat engine[3]. In Fig. 3(a), we plot the ratio  $\lambda_{\{n_i\}}(L_1, L_2)$  as a function of the interacting strength for different energy levels  $\{n_i\}$ . The curves for different energy levels show dips with different positions. For low temperature, since the particle occupation on higher energy levels can be neglected, we use two-level approximation to calculate the efficiency

$$\eta = 1 - \frac{\Delta_2}{\Delta_1}, \quad (14)$$

where only the ground state and the first excited state are considered with the energy gap  $\Delta_i = E_{(2,1)}^{(L_i)} - E_{(1,1)}^{(L_i)}$ ,  $i = 1, 2$ . Under the low temperature limit ( $T_2 = 2.5, T_4 =$

0.5 in Fig 3 (b) ), the efficiency derived with two-level approximation (black solid curve) matches with the exact numerical result (blue dots). For high temperature, the efficiency contains more contribution from high energy levels, and the efficiency approaches the ideal case  $1 - L_1^2/L_2^2$ .

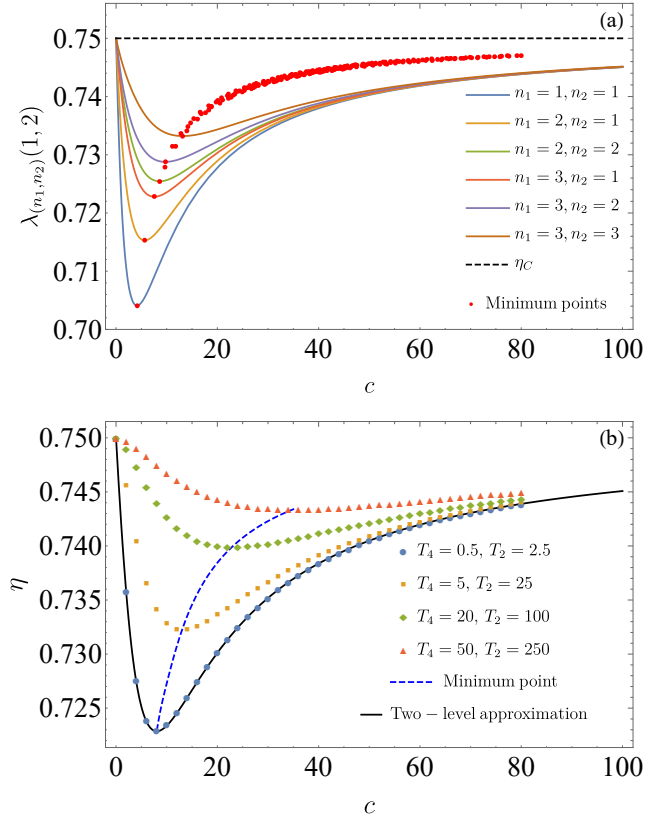


Figure 3. (Color online) (a) the ratio  $\lambda_{\{n_i\}}(L_1, L_2) = 1 - E_{\{n_i\}}^{(L_2)}/E_{\{n_i\}}^{(L_1)}$  with different interacting strength  $c$  for two interacting Bosons  $N = 2$ . We calculate the ratio for the state with the quantum number  $(n_1, n_2) = (1, 1), (1, 2), (1, 3), (2, 2), (2, 3), (3, 3)$ . The solid lines are the ratios for 6 corresponding energy levels, while the dashed line is the Carnot efficiency  $\eta_C = 1 - L_1^2/L_2^2 = 0.75$ . The red dots are the minimum point of the ratio, not only for the plotted energy levels but also including energy levels with higher energy. Fig.3 (b) shows the efficiency derived by numerical calculation for different temperature and two-state approximation result. They match well under low temperature limit  $T_4 = 0.5, T_2 = 2.5$ . The dots of different colors is the exact numerical result for different temperature, while the black solid line is derived by the two-level approximation from Eq. (14).

The efficiency of this Otto heat engine is affected by the temperature of the reservoirs, which is different from one-particle Otto heat engine. In Fig. (4), we study the temperature effect by modulating the temperature  $T_2$  of the hot reservoir from 50 to 250 with fixed temperature of the cold reservoir at  $T_4 = 8$ . Figure 4 (a) shows the efficiency  $\eta$  is larger for higher temperature

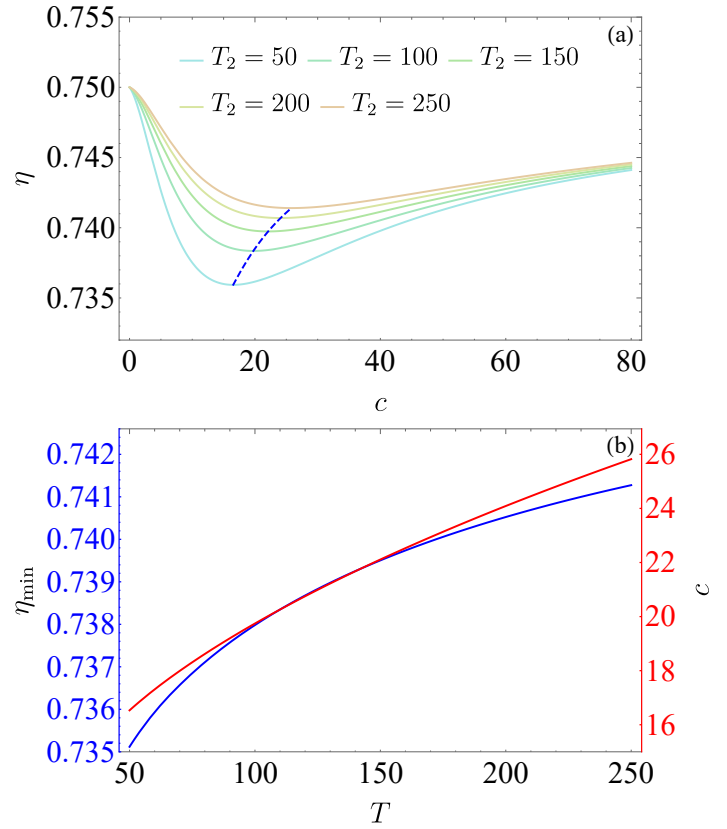


Figure 4. (Color online) The effect of temperature on the efficiency dip. The efficiency-interaction curve with different temperature of the hot reservoir  $T_2$ , modulating from 50 to 250. The temperature of the cold reservoir is fixed  $T_4 = 8$ . In Figure 4 (a), the solid lines of different colors represent the efficiency  $\eta$  for different temperature  $T_2$ . The blue dashed line shows the the minimum point of the instant efficiency for different temperature  $T_2$ . Figure 4 (b) extracts the coordinate of the minimum point for different  $T_2$  in Fig. 4. The blue line and the red line give the minimum efficiency  $\eta_{\min}$  and the interacting strength  $c$  for the the minimum point for different  $T_2$  respectively.

$T_2$  as expected. The minimum point of the efficiency for different temperature  $T_2$  is plotted with red dashed line. To figure out how the temperature  $T_2$  affects the minimum point of the efficiency, we plot both the efficiency  $\eta_{\min}$  and the interacting strength  $c$  of the minimum point with different temperature  $T_2$  in Figure 4 (b). The interacting strength  $c$  (the red line) and the efficiency  $\eta_{\min}$  (the blue line) for the minimum efficiency become larger when  $T_2$  increases, which matches the minimum point of  $\lambda_{\{n_i\}}(L_1, L_2)$  in Fig. 3. The behavior of the efficiency with different temperature  $T_2$  matches with the change of the ratio  $\lambda_{\{n_i\}}(L_1, L_2)$  of the corresponding energy levels.

#### IV. CONCLUSION

We have studied the quantum Otto heat engine with 1D repulsive Bose gas in a hard wall box to reveal the effect of interaction on the efficiency. For weak interaction, we conclude that the efficiency of the Otto heat engine is lower than the non-interacting case, smaller for high temperature and larger for low temperature. When the interaction is large, the efficiency recovers to its ini-

tial value, which is explained by the Bose-Fermi duality for 1D interacting Bose gas. By calculating the ratio  $\lambda_{\{n_i\}}(L_1, L_2)$ , we have explained the appearance of the minimum value of efficiency as the function of the interacting strength  $c$ . For the low temperature case, the Otto engine with the lowest two levels gives a good approximation with different interacting strength. For the high temperature case, the contribution for high levels shifts the minimum position as well as the corresponding efficiency.

- 
- [1] H. B. Callen, *Thermodynamics And An Introduction To Thermostatistics*, 2nd ed. (Wiley, 1985).
- [2] K. Huang, *Statistical mechanics*, 2nd ed. (Wiley, 1987).
- [3] H. T. Quan, Y. X. Liu, C. P. Sun, and F. Nori, *Phys. Rev. E* **76**, 031105 (2007).
- [4] H. Dong, D. Z. Xu, C. Y. Cai, and C. P. Sun, *Phys. Rev. E* **83**, 061108 (2011).
- [5] S. W. Kim, T. Sagawa, S. D. Liberato, and M. Ueda, *Phys. Rev. Lett.* **106**, 070401 (2011).
- [6] C. Y. Cai, H. Dong, and C. P. Sun, *Phys. Rev. E* **85**, 031114 (2012).
- [7] D. Gelbwaser-Klimovsky, W. Niedenzu, and G. Kurizki, in *Adv. At. Mol. Opt. Phy.* (Elsevier, 2015) pp. 329–407.
- [8] H. T. Quan, *Phys. Rev. E* **79**, 041129 (2009).
- [9] J. Bengtsson, M. N. Tengstrand, A. Wacker, P. Samuelsson, M. Ueda, H. Linke, and S. Reimann, *Phys. Rev. Lett.* **120**, 100601 (2018).
- [10] M. Gaudin, *Phys. Rev. A* **4**, 386 (1971).
- [11] M. T. Batchelor, X. W. Guan, N. Oelkers, and C. Lee, *J. Phys. A: Math. Gen.* **38**, 7787 (2005).
- [12] N. Oelkers, M. T. Batchelor, M. Bortz, and X.-W. Guan, *J. Phys. A: Math. Gen.* **39**, 1073 (2006).
- [13] D. Newman, F. Mintert, and A. Nazir, *Phys. Rev. E* **95**, 032139 (2017).
- [14] W. Hübner, G. Lefkidis, C. D. Dong, D. Chaudhuri, L. Chotorlishvili, and J. Berakdar, *Phys. Rev. B* **90**, 024401 (2014).
- [15] F. Altintas, A. U. C. Hardal, and Özgür E. Müstecaplıoğlu, *Phys. Rev. E* **90**, 032102 (2014).
- [16] G. Thomas and R. S. Johal, *Phys. Rev. E* **83**, 031135 (2011).
- [17] X. Huang, Q. Sun, D. Guo, and Q. Yu, *Physica A* **491**, 604 (2018).
- [18] K. Zhang, F. Bariani, and P. Meystre, *Phys. Rev. Lett.* **112**, 150602 (2014).
- [19] E. A. Ivanchenko, *Phys. Rev. E* **92**, 032124 (2015).
- [20] C. N. Yang, *Phys. Rev. Lett.* **19**, 1312 (1967).
- [21] M. Girardeau, *J. Math. Phys.* **1**, 516 (1960).